Proximal soil sensing-led management zone delineation for potato fields

Wenjun Ji[1, 2], Asim Biswas[3] *, Viacheslav Adamchuk[2], Isabelle Perron[4], Athyna Cambouris[4], Bernie Zebarth[5]

[1] Division of Precision Agriculture and Pedometrics, Department of Soil and Environment, Swedish University of Agricultural Sciences, Skara, Sweden SE-532 23
[2] Department of Bioresource Engineering, McGill University, 21111 Lakeshore Road, Ste-Anne-de-Bellevue, QC, Canada, H9X 3V9
[3] School of Environmental Sciences, University of Guelph, 50 Stone Road East, Guelph, ON, Canada, N1G 2W1
[4] Quebec Research and Development Centre, Agriculture and Agri-Food Canada, 2560 Hochelaga, Quebec City, QC, G1V 2J3
[5] Fredericton Research and Development Centre, Agriculture and Agri-Food Canada, 850 Lincoln Road, P.O. Box 20280, Fredericton, NB, E3B 4Z7

* Corresponding author: A. Biswas biswas@uoguelph.ca

A paper from the Proceedings of the
14th International Conference on Precision Agriculture
June 24 – June 27, 2018
Montreal, Quebec, Canada

Abstract. *A fundamental aspect of precision agriculture or site-specific crop management is the ability to recognize and address local changes in the crop production environment (e.g. soil) within the boundaries of a traditional management unit. However, the status quo approach to define local fertilizer need relies on systematic soil sampling followed by time and labour-intensive laboratory analysis. Proximal soil sensing offers numerous advantages over conventional soil characterization and has shown potential for management zone (MZ) delineation and site-specific crop management. While electromagnetic induction (EM) based sensors have been widely used, the use of spectroscopy-based sensors is still in its infancy. This study evaluated the capability of spectroscopy-based Veris P4000 soil sensor in predicting soil properties and two proximal soil sensors (EM-based DUALEM21S and Veris P4000) in delineating MZs from two commercial potato (Solanum tuberosum L.) fields from New Brunswick, Canada. The proximal sensor collected data (apparent electrical conductivity ECa and spectra) were then used to delineate MZs using the clustering method. The efficiency of the MZ delineation was then compared with the laboratory measured soil properties and the yield monitor data collected over three years. In total, 295 soil samples were collected and analyzed using standard laboratory procedures.*

DUALEM21S was used to map the ECa at four depths. Visible and near infrared (Vis-NIR) spectra (397-2212 nm wavelength) were collected in triplicate for all samples using the spectrometer from Veris P4000 system in laboratory conditions. The dataset was separated into calibration (70%) and validation subset (30%) and partial least square regression (PLSR) models with bootstrapping were developed and validated against laboratory measured soil properties. Spectroscopic system well predicted soil properties. It showed the strongest potential to predict soil organic matter (SOM) with the highest accuracy. Other soil properties that were either positively (e.g. Ca, Mg) or negatively correlated (e.g. pH, buffer pH) with SOM were also predicted with good accuracy. The point samples were then interpolated to field boundaries and used to develop MZs. The number of MZs were then optimized following the normalized classification entropy (NCE) and the fuzziness performance index (FPI). While lab measured physio-chemical properties identified three optimum MZs, the spectra predicted properties and DUALEM21S data identified two MZs. The choice of two MZs was consistent with the number of MZs identified from the yield monitor data. Clay content, soil moisture content and P concentration showed strongest correlations with yield variability among soil properties. DUALEM21S data from all four depths were strongly correlated with yield. In contrast, measured spectra showed relatively weak prediction (except principle component 1, PC1 and PC3) of yield. These results suggest that the EM based sensor was effective in delineating MZ, whereas more advancements are required to use spectra in MZ delineation.

Keywords. *Proximal soil sensing, management zones, soil spectroscopy, potato*

1. Introduction

The success of precision agriculture (PA) is dependent on the identification of local changes in the crop production environment (e.g. soil) through delineation of management zones (MZs) within the traditional management unit and then addressing them variably (site-specific crop management). However, the *status quo* approach of defining soil fertility variations and site-specific recommendations depend on traditional soil sampling followed by time and labor-intensive laboratory measurements. Proximal soil sensing (PSS) technologies (measure the properties of soils when they are in contact with, or at a relatively short distance (under 2 m) from the target) have potential as less expensive per unit of area technologies for detailed soil characterization. They offer numerous advantages over conventional soil characterization and management recommendations. Some static PSS systems can *in situ* measure relative soil information, which are then calibrated against laboratory measured data accurately and rapidly. These provide promising alternatives to conventional laboratory soil tests. One example of such PSS systems is the field scanners for soil cores (e.g. Kusumo et al., 2010; Cho et al., 2017). On the other hand, on-the-go sensors (e.g. Mouazen and Kuang, 2016) can collect fine-scale relative soil information over the study area from increased density of measurements at a relatively low cost and can be critical for variable rate and site-specific application recommendations in environmental monitoring and precision agriculture.

Various proximal soil sensors have been developed to measure different mechanical, physical and chemical soil properties based on electrical and electromagnetic, optical and radiometric, mechanical, acoustic, pneumatic and electrochemical measurement concepts (Adamchuk et al., 2004). Among these, electrical and electromagnetic sensors measure electrical resistivity/conductivity, capacitance or inductance as affected by soil. This could be done either using direct injection of electrical current into soil with contact electrodes, or by using electromagnetic induction without direct contact with soil. These sensors, paired with global navigation satellite system technology, have become the most attainable techniques for on-the-go mapping resulting from their rapid response, low cost and high durability. The main soil properties targeted with these sensors are soil texture (clay, sand and silt content), soil organic matter (SOM), moisture, salinity (Li et al., 2013), pH, cation exchange capacity (CEC) and soil depth variability (Mueller et al., 2003). Optical sensors use different portions of electromagnetic waves to detect the level of energy absorbed/reflected by soil. Electromagnetic radiation consists of vast range of wavelengths and frequencies, including gamma-ray, X-ray, ultraviolet, visible, near-infrared and mid-infrared, micro waves and radio waves. Ultraviolet/visible/infrared measurement techniques are based on diffuse reflectance (or atomic emission) spectroscopy and offer soil measurements that are rapid, relatively inexpensive, safe and non-invasive. Visible-near

infrared (vis-NIR) diffuse reflectance spectroscopy with a wavelength range of 350-2500 nm has gained a tremendous attention as it can simultaneously predict multiple soil properties with a single scan or data collection. Basically, one scans soil samples using Vis-NIR and develop mathematical models against laboratory measurements. These techniques have been used to measure soil organic matter/carbon (Viscarra Rossel et al., 2007; Viscarra Rossel et al., 2006; Shi et al., 2015), heavy metal contaminants (Kalnicky and Singhvi, 2001), soil clay (Viscarra Rossel et al., 2009) and sand content (Guillou et al., 2015), moisture (Mouazen et al., 2006), pH (Ji et al., 2014), nitrate or nitrogen content (Kuang & Mouazen, 2011), CEC and other properties.

Delineation of MZs is the subdivision of fields into parts with similar soil conditions or properties with an intention of managing the zones similarly but differently from other zones (Peralta and Costa 2013). It can be defined as "a sub-region of a field that expresses a relatively homogeneous combination of yield-limiting factors for which a single rate of a specific crop input is appropriate". MZ delineation entails thematic mapping of potential yield-limiting parameters and classifying them into subfields (Corwin and Lesch, 2010). The methodology varies in degree of complexity, but the fundamental procedure involves collection of one or more variables related to yield, thematic mapping of variables, chiefly employing geostatistical methods, and ultimately classification of one or more variables into zones using one of many various clustering algorithms or numerical techniques. However, there are a series of challenges in identifying MZs arising from complex correlation of underlying controlling factors, strong spatial variability of soil properties and nutrient concentrations (Peralta and Costa, 2013). Nonetheless, the inability to obtain soil characteristics rapidly and inexpensively remains one of the biggest limitations for MZ delineation (Adamchuk et al., 2004). While approaches such as intensive soil sampling, a time-consuming and costly (Shaner et al., 2008) approach limited to point measurements (Toy et al. 2010), are often not practical for high resolution measurements and thus identification of MZs. In contrast, proximal soil sensors can provide high resolution information on soil variability and shown potential for delineating MZs. Therefore, the objectives of this study were to 1) evaluate the capability of spectroscopy-based Veris P4000 proximal soil sensor in predicting soil properties from two commercial potato (*Solanum tuberosum* L.) fields from New Brunswick, Canada; and 2) use the spatial distribution of soil properties, sensor data and yield to delineate MZs for site-specific management.

2. Materials and methods

2.1 Site description and soil sampling

Two commercial potato fields were selected for this study from New Brunswick, Canada (Fig. 1). The fields are under intensive potato production. One field is 21 ha in size (Field1) and another is 18 ha in size (Field2). Soils of Field1 are good to poorly drained, sandy loam to clay loam, and of glacial till origin and was classified as Holmesville (Orthic Ferro-Humic Podzol), Undine (Orthic Humo-Ferric Podzol), Johnville (Gleyed Humo-Ferric Podzol) and Siegas (Brunisolic Gray Luvisol) (Langmaid et al. 1980). Soils of Field2 were classified as Caribou (Podzolic Gray Luvisol) and Carleton (Orthic Humo-Ferric Podzol) soil series, which are moderately well drained, loam to silt loam, and of glacial till origin (Fahmy and Rees, 1996). Soil of both fields had a gravel content of about 15-35% and soil depth varied between 0.65 and 1.00 m (Milburn et al., 1989). The long-term average annual precipitation of Field1 and Field2 are 1099 and 966 mm, respectively with mean growing season precipitation of 640 and 600 mm, respectively (Environment Canada, 2016).

A field sampling campaign was carried out in September 2015 following a triangular grid sampling design with a spacing of 33 m within the center 12 ha of the field and 71 m close to two long-end or the rest of the fields (Fig. 1). Composite surface soil samples from 0-15 cm depth were collected within 1.5 m radius of the sampling points pre-determined using ArcGIS. A total of 154 samples for Field1 and 141 samples from Field2 were collected using an auger and a series of soil physiochemical properties (moisture content, particle sizes (selected samples to a total of 41 and 37 for Field1 and Field2, respectively), total carbon, total nitrogen, pH, P, K, Ca, Mg, Fe, Mn, Zn, Cu, and Al) were analyzed in laboratory following standard laboratory protocol.

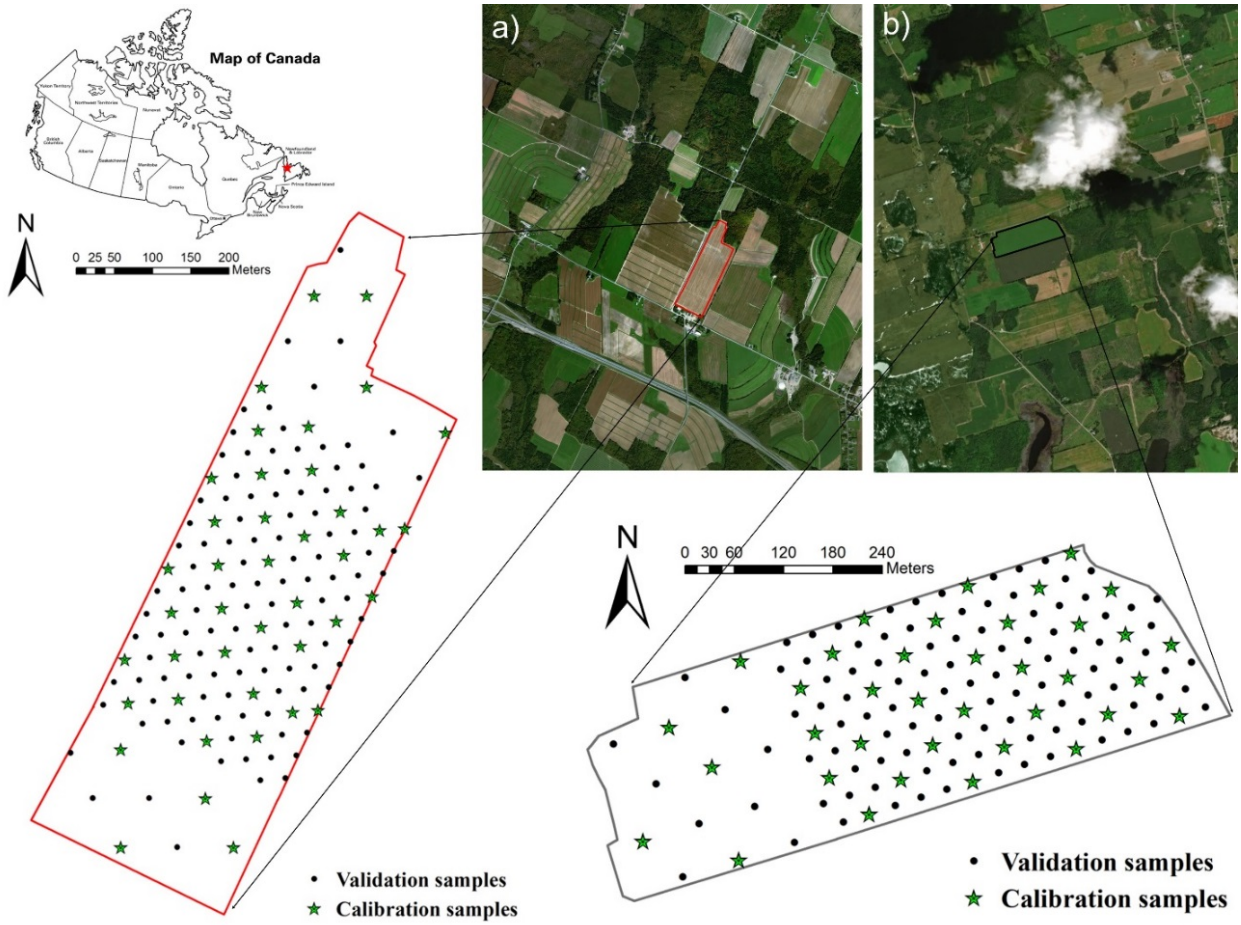

Fig. 1: Study site showing two fields; a) Field1 and b) Field2 with sampling points for calibration and validation of predictive relationships for spectroscopic measurements.

2.2 Field mapping using proximal soil sensors

Both fields were intensively mapped using DUALEM21S (Dualem, Inc., Milton, Ontario, Canada) (Fig. 2) based on electromagnetic induction principle. Soils from selected locations were scanned using Veris P4000 (Veris P4000, Veris Technologies, Inc., Salina, Kansas, USA) multi-sensor platform based on spectroscopic principles. DUALEM21S was equipped with a real-time kinematic (RTK) AgGPS 542 global navigation satellite system (GNSS) receiver (Trimble RTK/PP-4700 GPS, Trimble Navigation Limited, Sunnyvale, CA, USA) to record precise location and the elevation.

DUALEM21S has dual-geometry receivers at separations of 1- and 2-m from the transmitter providing simultaneous measurements of four (two with horizontal co-planar (HCP) and two with perpendicular (PRP) geometries) ECa soundings at different depths. The receiving coils provided information on HCP at 1 m (HCP1) and 2 m (HCP2) distances from the transmitter and PRP at 1.1 m (PRP1) and 2.1 m (PRP2) distances from the transmitter. The effective sensing depth (75% response) of HCP1, HCP2, PRP1, and PRP2 were 1.55 m, 3.18 m, 0.54 m, and 1.03 m, respectively (Mat Su et al., 2009). The equipment was pulled by an all-terrain vehicle in parallel lines of about 10 m separation. The data from the DUALEM-21s and the Trimble RTK were logged using a custom DUALEM_DAQ logging software (Ji et al., 2017).

Veris P4000 is a commercial multi-sensor platform and was used to collect vis-NIR reflectance spectra (350-2200 nm with 8 nm resolution) in laboratory (Fig. 2). Soil spectra in triplicate were collected for surface soil samples, processed and averaged before developing predictive relationship. Savitzky-Golay algorithm with a window size of 11 nm and a polynomial of order 2, and mean centering were applied to the raw spectra as pre-treatment before performing further analysis.

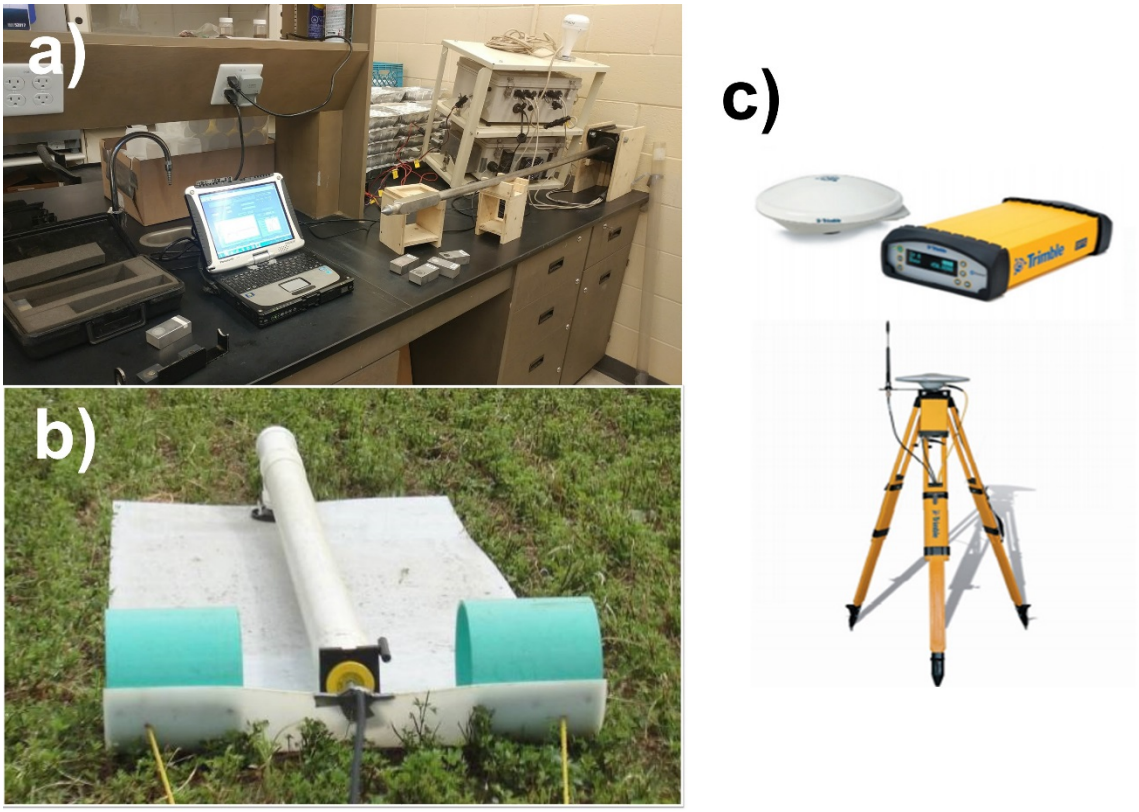

Fig. 2: a) Veris P4000 multi-sensor platform, b) DUALEM21S and c) RTK GPS with receiving station.

2.4 Tuber yield data collection

Yield data for Field1 were collected for 3 years (2013, 2014, and 2016) and Field2 for 2 years (2014 and 2016) using the RiteYield yield monitor system (Greentronics, Elmira, ON, Canada) attached to harvesters. Field1's yield data were collected along a row width of 15 m (16 row harvester) and Field2's yield data were collected along a row width of 11 m (12 row harvester). The harvesters were also equipped with RTK GPS systems (Trimble Navigation, Inc.) and the yield monitors were calibrated at the beginning of the season.

2.3 Data analysis

All the laboratory measured soil properties were interpolated using ordinary kriging in R computing language (R 3.3.3, R Development Core Team, 2017). Similarly, the yield monitor data as well as other proximal soil sensing data were also interpolated, and all the interpolated maps were harmonized in terms of spatial resolution (Fig. 3). In addition, proximal soil sensor as well as yield monitored data at the sampling points were extracted from the interpolated maps for developing prediction models. The spectral data were decomposed using principle component analysis (PCA) and the top 5 principle components (PCs) contributing more than 99.9% of the total variance were considered to develop predictive models. The correlation between and among soil properties, proximal soil sensors and yield were quantified using Pearson correlation coefficient. Additionally, to test the validity of spectroscopic data, the predictive capability of soil spectra for the lab measured properties were examined. Predictive models were developed for all soil properties in relation to average soil spectra of 0-15 cm using partial least square regression (PLSR) (Fig. 3). The accuracy of prediction was assessed based on root mean square error (RMSE) and coefficient of determination (R2).

Spatial layers of soil properties were used to delineate MZs using an unsupervised Fuzzy classification algorithm. MZs were delineated individually for spatially interpolated soil properties, spatially interpolated layers of soil ECa measurement using DUALEM21S, spatially interpolated layers of 5 PCs derived from soil spectral measurements and spatially interpolated yield monitor data to compare the efficacy of using certain sensors compared to the yield response of the field

(Fig. 3). The MZs delineated using various methods were then compared with each other to examine the persistency in measurement (Fig. 3). The number of optimum MZs were decided based on two criteria; normalized classification entropy (NCE) and the fuzziness performance index (FPI). The NCE models the amount of disorganization created by dividing a data set into classes. The best classification is determined where NCE reaches a minimum. Similarly, the FPI models the amount of membership sharing that occurs between classes. Like the NCE, the best classification is determined where FPI reaches a minimum.

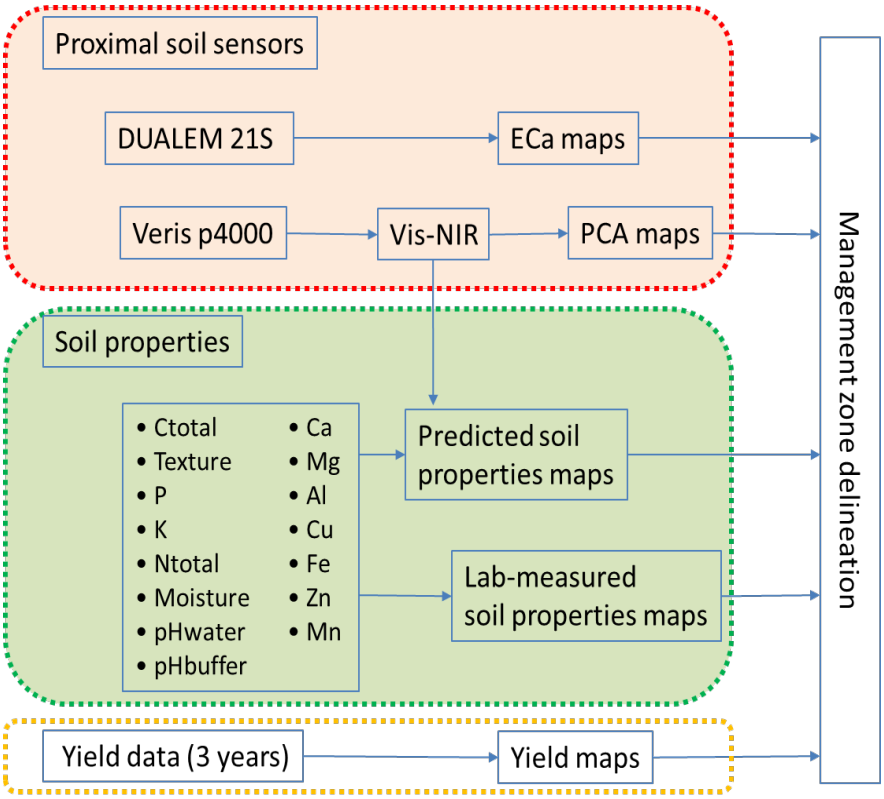

Fig. 3. Outline of the steps of data analysis and MZ delineation

Though all the analyses were performed for both fields, for the brevity of the paper, results form only one field is presented here as a case study. Therefore, all the results and discussion will be focused on one field; Field1 for the rest of the manuscript.

Table 1: Descriptive statistics of soil properties for Field1 samples

Soil properties	Average	Standard deviation	Coefficient of Variation %	Minimum	Maximum
pH	5.84	0.39	7	5.19	7.15
Soil water %	24.4	4.00	16	14.0	36.5
Total C mg kg^{-1}	2.1	0.24	11	1.13	2.82
Total N mg kg^{-1}	0.2	0.02	12	0.11	0.37
P mg kg^{-1}	238.36	57.39	24	67.94	357.87
K mg kg^{-1}	183.27	43.35	24	104.84	335.6
Ca mg kg^{-1}	808.97	259.95	32	350.83	1693.02
Mg mg kg^{-1}	115.85	44.51	38	50.16	285.35
Al mg kg^{-1}	1813.95	111.63	6	1438.89	1999.02
Cu mg kg^{-1}	3.91	1.28	33	1.57	6.91
Fe mg kg^{-1}	316.46	51.43	16	176.19	478.68
Zn mg kg^{-1}	2.89	0.58	20	1.59	4.2

Mn mg kg^{-1}	39.17	14.3	37	19.62	143.58
Clay mg kg^{-1}	151	25	16	119	210
Silt mg kg^{-1}	508	52	10	382	609
Sand mg kg^{-1}	341	73	22	190	483
Gravel mg kg^{-1}	237	67	28	73	411
Elevation m	214.3	3.5	2	205.6	220.9
$Yield_{2013}$ Mg ha^{-1}	40.5	10.4	26	6.5	70
$Yield_{2014}$ Mg ha^{-1}	36.9	10.3	28	3	62.5
$Yield_{2016}$ Mg ha^{-1}	34.2	7.3	21	15.7	55.9

3. Results and discussion

3.1 Spatial variability of soil properties and yield

Soil properties varied within the field (Table 1). Almost all the soil properties except pH and Al exhibited coefficient of variation (CV) larger than 10%. CV as high as 38% was observed for Mg. A similar high variability was observed for Mn (37%), Cu (33%) and Ca (32%). Strong variability was also observed in soil particle sizes. Variability in the particle sizes may be attributed to the variability in soil classes as classified in earlier survey (Langmaid et al., 1980). A year-to-year variation in potato production was observed for the same field. In 2013, the tuber yield was 40.5 Mg ha^{-1}. However, a decreasing yield pattern was observed in 2014 (36.9 Mg ha^{-1}) and in 2016 (34.2 Mg ha^{-1}). Year to year variation in climatic conditions might have contributed to the variability and the decreasing pattern in tuber yield.

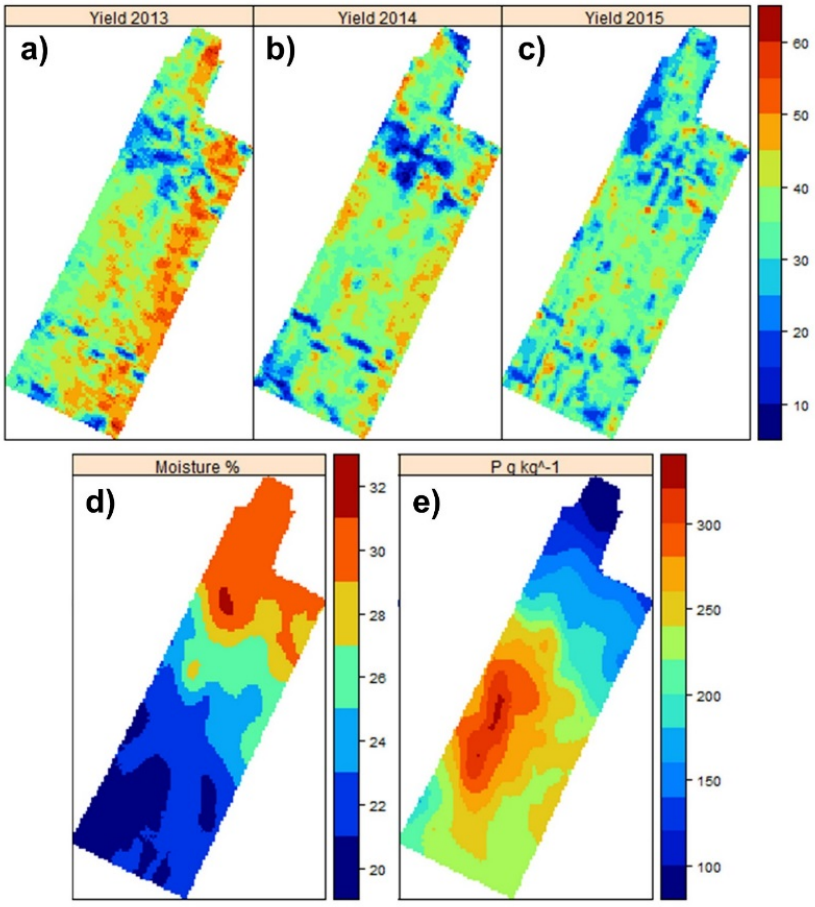

Fig. 4: Spatial distribution of yield (Mg ha^{-1}) in a) 2013, b) 2014, and c) 2016, and the spatial distribution of d) soil moisture (%) and P (g kg^{-1}).

The variability was also visible in the spatial distribution of soil properties (Fig. 4). For example, an increasing pattern of soil moisture was observed from southern part (~20%) to the norther part (~32%) of the field. Similarly, variability in the spatial distribution of soil P was observed with the highest amount in the center part of the field and decreasing at the lowest level in the northern most part of the field. Often, the center part of the field is used to initially store the manure before application and might have contributed to the higher amount of P. Similarly, a year-to-year variability in the spatial distribution of yield was also observed (Fig. 4) but with a consistent trend. For example, an area close to the northern part consistently exhibited lower yield than rest part of the field (Fig. 4). Though the trend in the spatial distribution in yield was not visible in the spatial distribution of majority of soil properties, a moderate linear correlation was observed between most of the soil properties and yield (discussed later).

3.2 Spatial variability of sensor measurements

A strong spatial variability in the proximal soil sensors measurements were also observed (Fig. 5). For example, the first PC (contributing 83.8% of the total variance) of spectral measurements was highly variable throughout the field. As the variance contribution decreased, the spatial variability also decreased. However, a small point with high variability was observed at the northern corner of the field in PC3. Similarly, a stronger variability was also observed at the same location in the distribution of DUALEM21S measurements (Fig. 5). The pattern in the spatial distribution of soil ECa showed similar patterns as seen in the spatial distribution in tuber yield. Basically, high ECa values were attributed to the lower yield (Fig. 4a-c). Spatial similarity in the distribution of yield and DUALEM21S measurements were also visible in the correlation (Fig. 6). Spatial variability in the yield was visible neither in the spatial distribution of soil properties nor in the spatial distribution of soil spectral measurements (Fig. 6).

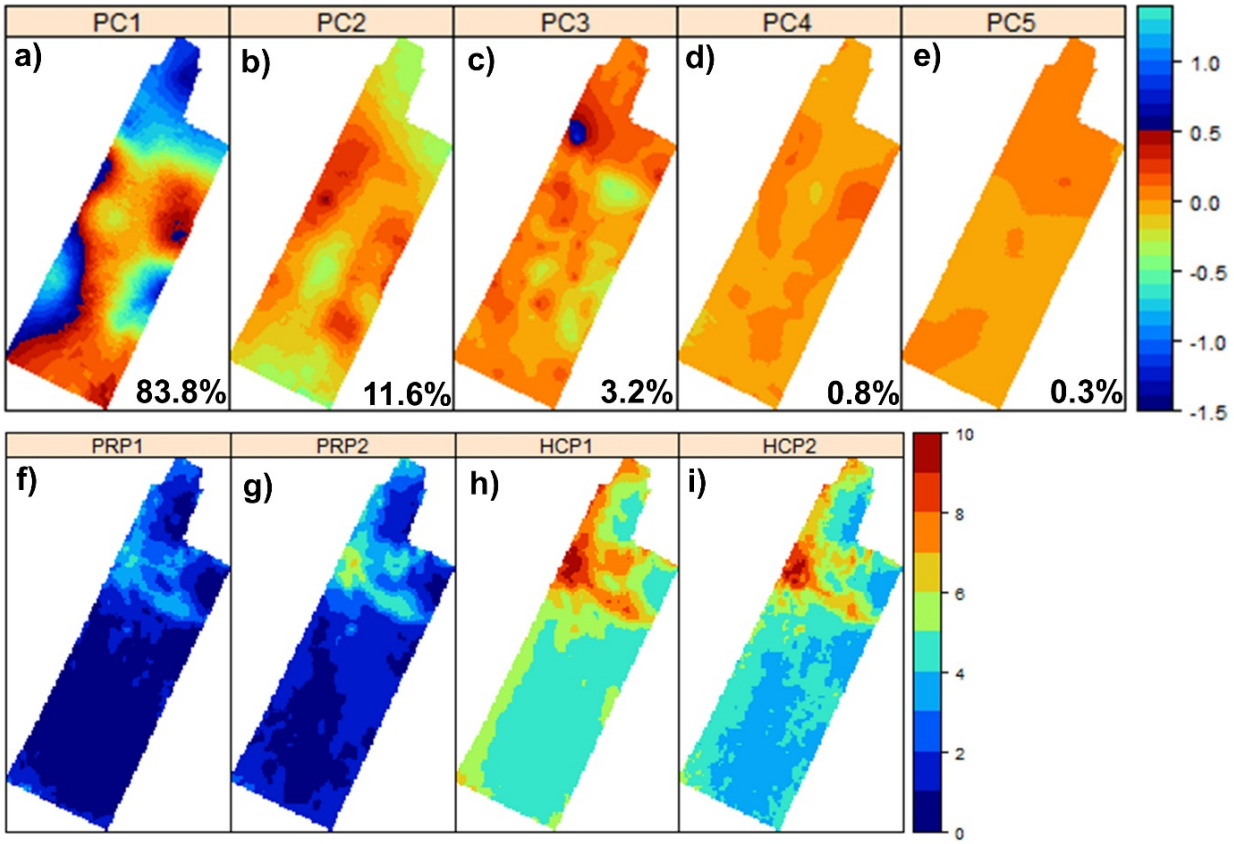

Fig. 5. Spatial distribution of proximal soil sensor measurements. a-e) show spatial distribution of PC1-PC5, respectively with their variance contribution towards the total variance and f-i) show the spatial distribution of soil ECa measured using DUAMEM21S at 4 different depths.

3.3 Correlation between and among soil properties, sensor measurements and yield

A variable correlation was observed among and between soil properties, proximal soil sensor data and yield (Fig. 6). For example, most of the soil properties were moderately correlated with yield particularly the yield of 2016 (Fig. 6). The correlation between soil properties and yield was observed in an increasing fashion from 2013 to 2016 except Fe, which showed a decreasing correlation. A strong negative correlation was observed between yields and DUALEM21S sensor data. This may be that the high salt concentration affected the yield negatively. A strong positive correlation between PC5 and the DUALEM21S sensor data were also observed. Similarly, a strong correlation was observed between DUALEM21S sensor data layers and majority of soil properties. For example, soil particle sizes showed strong correlation with DUALEM21S sensor layers. While clay and silt showed positive correlation, sand showed negative correlation with DUALEM21S sensor data. Higher surface area in smaller size particles (clay and silt) contributed to the higher exchange capacity and higher salt concentration in soil leading to positive correlation, while sand exhibited opposite relationship.

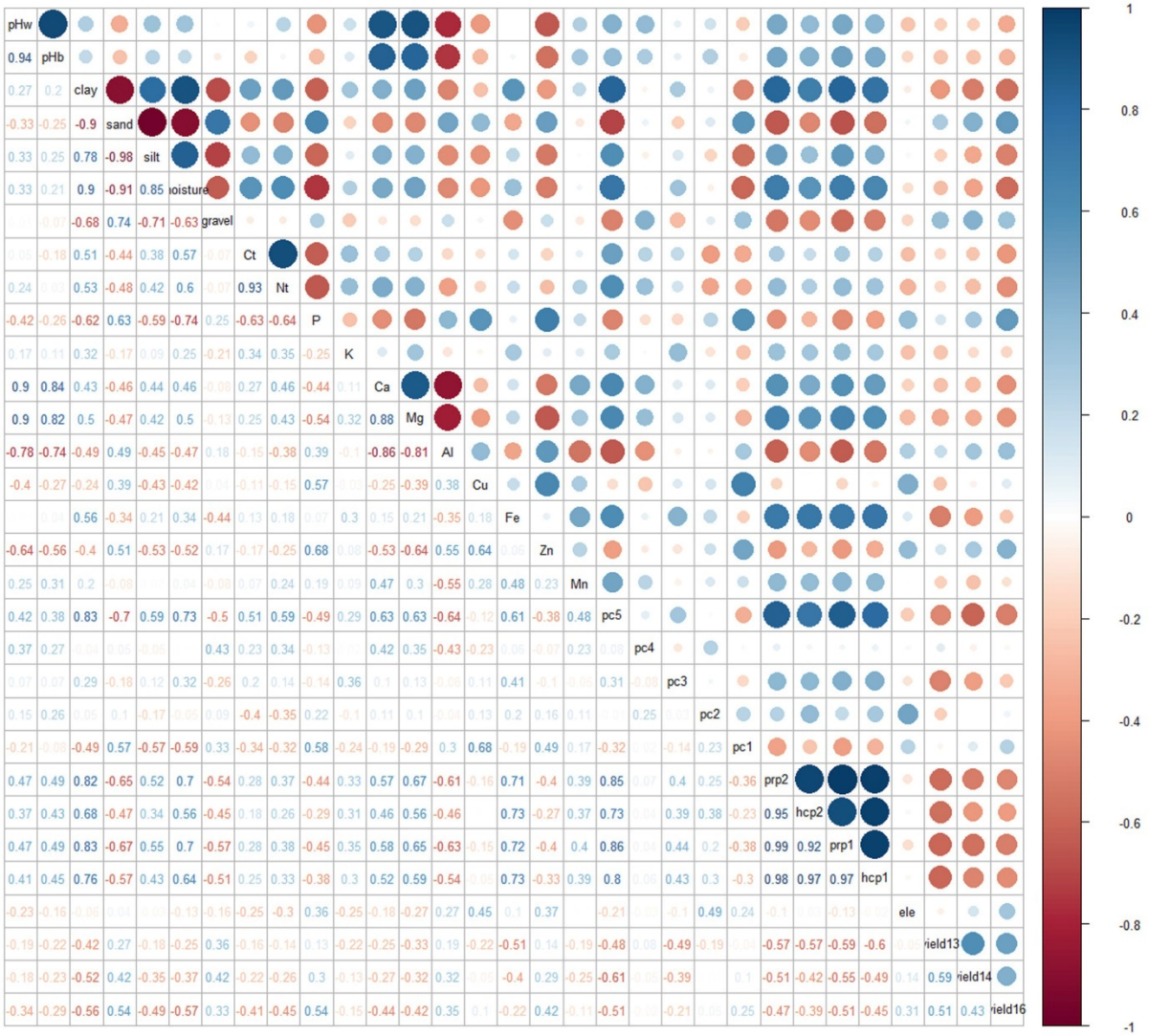

Fig. 6: Correlation coefficients between and among soil properties, proximal soil sensors data layers, and yield. While the size of the circle indicates the strength of the correlation, the color indicates the type of relationship (positive and negative).

Among the soil properties, soil particle sizes were highly correlated among each other. Similarly, a strong correlation was observed among the cations (Fig. 6). An obvious strong negative correlation was also observed between soil Al and Ca and Mg. A negative correlation between

DUALEM21S sensor data and Al may be attributed to the contribution of higher Al towards the acidity and unavailability of cations leading to lower cationic concentrations.

3.4 Spectroscopic prediction of soil properties

A predictive relationship was developed between lab-measured soil properties and average spectral signature of the top 0-15 cm layer using PLSR. Figure 6 shows the scatter plots between lab measured and spectral predicted soil properties. Majority of the soil properties exhibited good agreement between the lab measured and predicted soil properties. Calibration and validation R2 values >0.50 are marked with 'smiley' faces in Fig. 7. Basically, clay, sand, total C, total N, water and buffer pH, P, Zn, Al and Ca had correlation >0.50 for both calibration and validation samples with as high as 0.80 for clay and Al and 0.83 for Ca in calibration samples. This showed that the spectroscopic techniques could be used to predict soil properties and could be used to fast characterize soil properties.

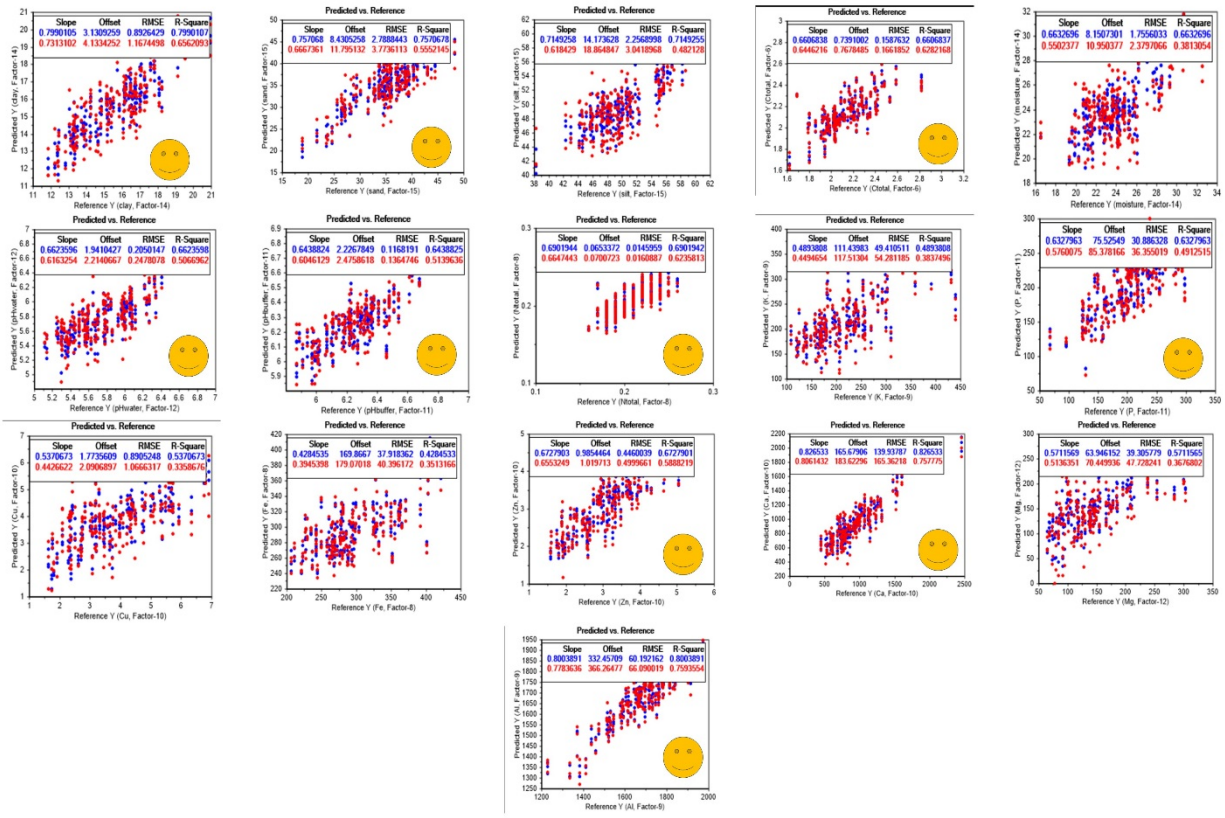

Fig. 7: Spectroscopic prediction of soil properties. The red dots indicate the calibrations samples and blue dots indicate the validation samples. Slope, offset, RMSE and R2 for each prediction are indicated in each sub-figure. The parameters are; top row from left to right- clay, sand, silt, total C and moisture; 2nd row from left to right- water pH, buffer pH, total N, K, and P; 3rd row from left to right- Ca, Fe, Zn, Cu and Mg; bottom row- Al. Strong prediction for soil properties are marked with a smiley face ☺.

3.5 Delineation of management zones

MZs were delineated (Fig. 3) using a series of spatial distribution maps of soil properties, proximal soil sensors and yield maps. The optimum number of MZ were decided based on the minimum value of NCE and FPI. An optimum number of MZ were identified to be 3 when spatial distribution maps of all soil properties were used (Fig. 8). A clear demarcation of three zones; northern part, middle part and southern part of the field indicated operational feasibility. However, as the number of MZ were increased, the scatterness of the zones indicated difficulty in operation and management (Fig. 8).

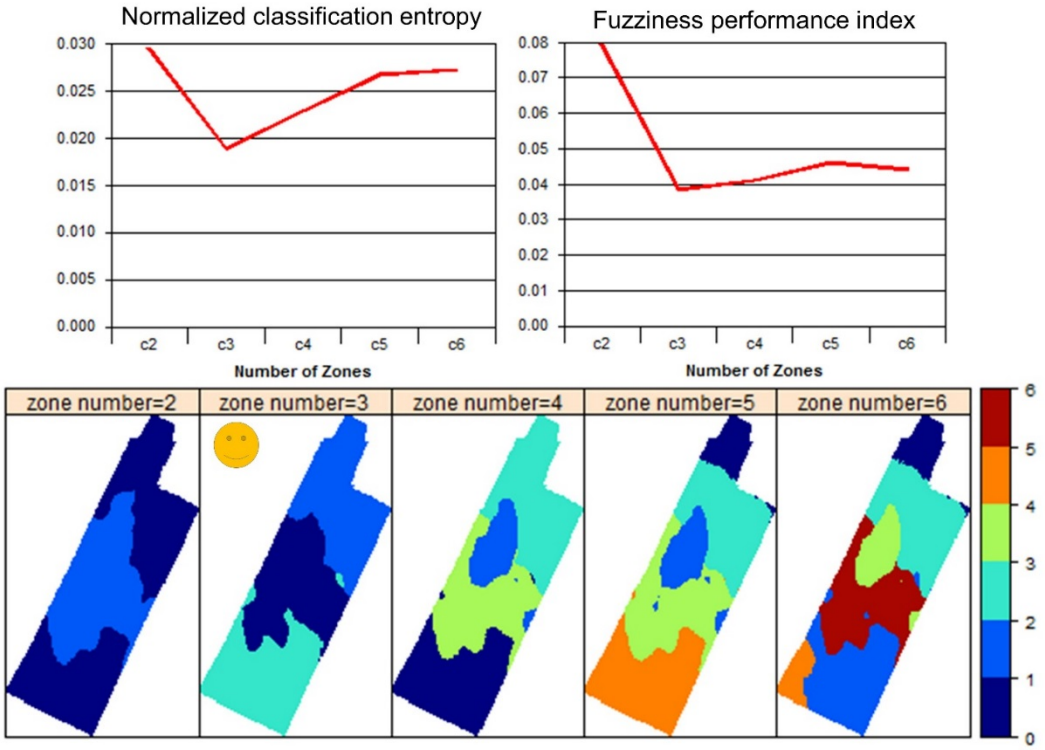

Fig. 8: Management zones delineated using the spatial distribution maps of soil properties (bottom row). The optimum number of zones were identified based on minimum NCE and FPI value (top row).

However, when the DUALEM21S sensor data layers were used to delineate MZs, 2 MZs were identified to be optimum (Fig. 9). A clear demarcation of the northern part of the field to the bottom/southern of the field represented the variability in the spatial distribution maps of sensor layers (Fig. 5). However, as the number of MZs were increased, the scatterness in the MZs visibly showed the difficulty in management. Similarly, 2 MZs were identified to be optimum using the spatial distribution maps of PCs of spectral measurements from Veris P4000 (Fig. 10). However, 2 MZs identified using Veris P4000 data were not like the MZs identified from the DUALEM21s. Separation of sections of MZs clearly indicated the difficulty in variably managing the field. This became more problematic with the increase in the number of MZs with highly scattered sections of MZs throughout the field (Fig. 10), though the spatial variability in the PCs of spectral measurements was not that strong (Fig. 5). A same number of MZs (two) were also identified when using yield monitor data of three years (2013, 2014 and 2016) (Fig. 11). However, non-coherent locations of MZs will make the management difficult compared to the MZs separated using DUALEM21S sensor. This clearly showed the superiority of using proximal soil sensors in delineating MZs that will be easy to manage.

4. Conclusions

This study examined the feasibility of proximal soil sensors for delineating management zones for site-specific management of potato, a high value crop. An electromagnetic induction based proximal soil sensor (DUALEM21S) and a spectroscopy-based proximal soil sensor (commercial multi-sensor platform Veris P4000) were used to map two commercial potato fields. Soil samples were also collected following a grid sampling strategy and measured in laboratory for a series of soil properties. The feasibility of predicting those soil properties using spectroscopy-based measurements were tested. A strong agreement was observed between most of the laboratory measured and spectral predicted soil properties showing potential for fast characterization of soil.

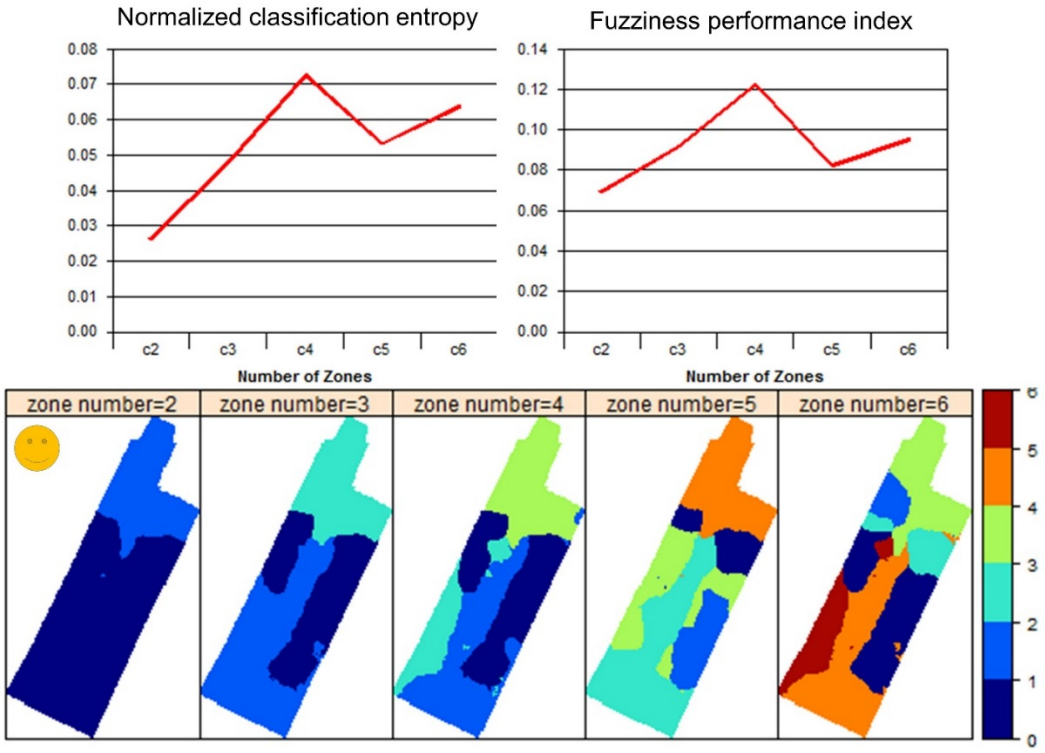

Fig. 9: Management zones delineated using the spatial distribution maps of DUALEM21S sensor data layers (bottom row). The optimum number of zones were identified based on minimum NCE and FPI value (top row).

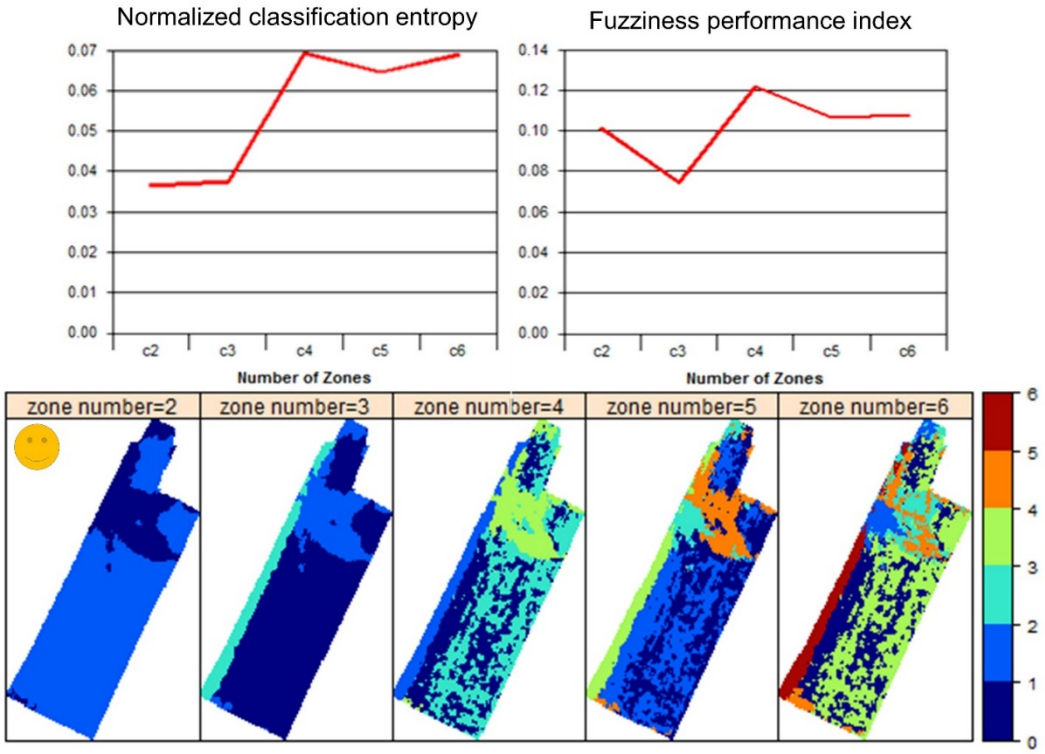

Fig. 10: Management zones delineated using the spatial distribution maps of principle components of spectral signatures collected using Veris P4000 (bottom row). The optimum number of zones were identified based on minimum NCE and FPI value (top row).

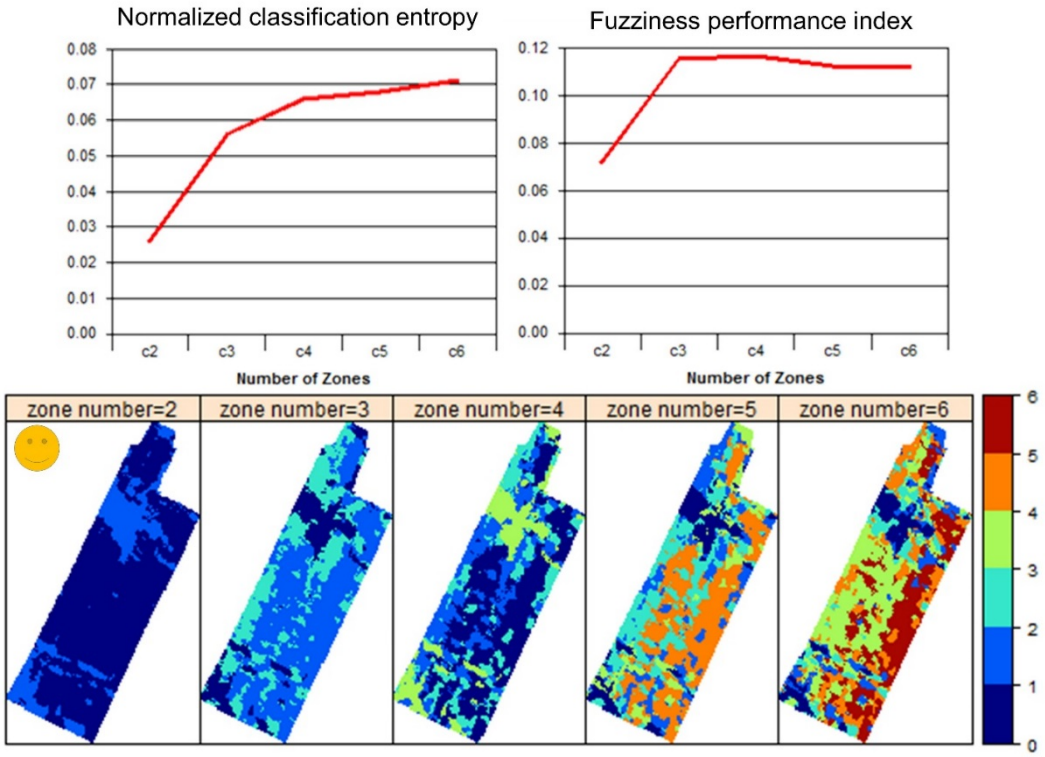

Fig. 11: Management zones delineated using the spatial distribution maps of yield from 2013, 2014 and 2016 (bottom row). The optimum number of zones were identified based on minimum NCE and FPI value (top row).

Further, the spatial distribution of soil properties measured in laboratory, spatial distribution of soil ECa measured using DUALEM21S, spatial distribution of principle components derived from spectral measurements and the spatial distribution of yield data were used to delineate MZs following a clustering algorithm. The number of zones were optimized based on two statistical criteria; normalized classification entropy and fuzziness performance index. While three MZs based on spatial distribution of soil properties were found to be optimum, two MZs were found to be optimum for all other data used. Among these, DUALEM21S provided a comprehensive and spatially co-located MZs, which showed improved feasibility for site-specific management over other methods. Spectroscopy-based proximal soil sensor showed potential in predicting soil properties, while the MZs delineated may not provide the best information and need further exploration.

Acknowledgments

This project was funded by grants to Asim Biswas NSERC (Natural Sciences and Engineering Research Council of Canada, RGPIN-2014-04100) and the AgriInnovation Program of Agriculture and Agri-Food Canada (AAFC) to Athyna Cambouris. The authors would like to thank Sarah-Maude Parent, Claude Lévesque, Ginette Decker, Kyle MacKinley, Gilles Moreau (McCain Foods Canada) and Gordon Fairchild (Eastern Canada Soil and Water Conservation Centre) for their field work and laboratory support.

References

Adamchuk, V.I., Hummel, J.W., Morgan, M.T., and Upadhyaya, S.K. (2004). On-the-go soil sensors for precision agriculture. *Computers and Electronics in Agriculture* **44**, 71-91.

Cho, Y., Sudduth, K.A., and Drummond, S.T. (2017). Profile soil property estimation using a vis-NIR-EC-force probe. Transactions of ASABE **60**, 683-692.

Corwin, D.L., and Lesch, S.M. (2010). Delineating Site-Specific Management Units with Proximal Sensors.

Pages 139–165 in M. A. Oliver, ed. *Geostatistical Applications for Precision Agriculture*. Springer Netherlands, Dordrecht.

Environment Canada. 2016. Canadian Climate Normals, 1981-2010 Climate Normals & Averages. [Online] Available: http://climate.weather.gc.ca/climate_normals/

Fahmy, S.H. and Rees, H.W. (1996). Soils of the Woodstock–Florenceville area, Carleton County, New Brunswick. Research Branch, Agriculture and Agri-Food Canada, Ottawa, ON.

Guillou, F.L., Wetterlind, W., Viscarra Rossel, R.A., Hicks, W., Grundy, M., and Tuomi, S. (2015). How does grinding affect the mid-infrared spectra of soil and their multivariate calibrations to texture and organic carbon? *Soil Research* **53**, 913-921.

Ji, W., Adamchuk V, Lauzon S, et al. (2017). Pre-processing of on-the-go mapping data. Pedometrics 2017, Wageningen, Netherlands, June 26th to July 1st.

Ji, W., Shi, Z., Huang, J., and Li, S. (2014). In situ measurement of some soil properties in paddy soil using visible and near-infrared spectroscopy. *PLoS One* **9**, e105708.

Kalnicky, D.J., and Singhvi, R. (2001). Field portable XRF analysis of environmental samples. *Journal of Hazardous Materials* **83**, 93-122.

Kuang, B., and Mouazen, A.M. (2011). Calibration of visible and near infrared spectroscopy for soil analysis at the field scale on three European farms. *European Journal of Soil Science* **62**, 629-636.

Kusumo, B.H., Hedley, M.J., Tuohy, M.P., Hedley, C.B., and Arnold, G.C. (2010). Predicting Soil Carbon and Nitrogen Concentrations and Pasture Root Densities from Proximally Sensed Soil Spectral Reflectance. In: R.A. Viscarra Rossel, A.B. McBratney, B. Minasny (Eds.), *Proximal Soil Sensing*. Springer Netherlands, Dordrecht, pp. 177-190.

Langmaid, K., MacMillan, J. and Losier, J. (1980). Soils of Madawaska County. New Brunswick Res Branch, Canada Dep of Agric and New Brunswick Dep of Agric, Fredericton, NB.

Li, H.Y., Shi, Z., Webster, R., and Triantafilis, J. (2013). Mapping the three-dimensional variation of soil salinity in a rice-paddy soil. *Geoderma* **195-196**, 31-41.

Milburn, P., Rees, H., Fahmy, S. and Gartley, C. (1989). Soil depth groups for agricultural land development planning in New Brunswick. *Canadian Agricultural Engineering,* **31**, 1–5.

Mouazen, A. M., and Kuang, B. (2016). On-line visible and near infrared spectroscopy for in-field phosphorous management. *Soil and Tillage Research*, **155**, 471-477.

Mouazen, A.M., Karoui, R., De Baerdemaeker, J., and Ramon, H. (2006). Characterization of Soil Water Content Using Measured Visible and Near Infrared Spectra. *Soil Science Society of America Journal*. **70**, 1295-1302.

Mueller, T.G., Hartsock, N.J., Stombaugh, T.S., Shearer, S.A., Cornelius, P.L., and Barnhisel, R.I. (2003). Soil electrical conductivity map variability in limestone soils overlain by loess. *Agronomy Journal* **95**, 496-507.

Peralta, N. R. and Costa, J. L. (2013). Delineation of management zones with soil apparent electrical conductivity to improve nutrient management. *Computers and Electronics in Agriculture* **99,** 218–226.

Shaner, D. L., Khosla, R., Brodahl, M. K., Buchleiter, G. W. and Farahani, H. J. (2008). How Well Does Zone Sampling Based on Soil Electrical Conductivity Maps Represent Soil Variability? *Agronomy Journal* **100,** 1472–1480.

Shi, Z., Ji, W., Viscarra Rossel, R.A., Chen, S., and Zhou, Y. (2015). Prediction of soil organic matter using a spatially constrained local partial least squares regression and the Chinese vis–NIR spectral library. *European Journal of Soil Science* **66**, 679-687.

Toy, C. W., Steelman, C. M. and Endres, A. L. (2010). Comparing electromagnetic induction and ground penetrating radar techniques for estimating soil moisture content. *Proceedings of 13th International Conference on Ground Penetrating Radar.*

Viscarra Rossel, R.A., Cattle, S.R., Ortega, A., and Fouad, Y. (2009). In situ measurements of soil colour, mineral composition and clay content by vis–NIR spectroscopy. *Geoderma* **150**, 253-266.

Viscarra Rossel, R.A., McGlynn, R.N., and McBratney, A.B. (2006). Determining the composition of mineral-organic mixes using UV–vis–NIR diffuse reflectance spectroscopy. *Geoderma* **137**, 70-82.

Viscarra Rossel, R.A., Taylor, H.J., and McBratney, A.B. (2007). Multivariate calibration of hyperspectral γ-ray energy spectra for proximal soil sensing. *European Journal of Soil Science* **58**, 343-353.